Russian Journal of Inorganic Chemistry, Vol. 42, No. 1, 1997, pp. 103–109. Translated from Zhurnal Neorganicheskoi Khimii, Vol. 42, No. 1, 1997, pp. 110–117.

186

PHYSICAL METHODS OF INVESTIGATION

Thermodynamics and Kinetics of MSi_2 Formation under Shock Compression

S. S. Batsanov*, S. M. Gavrilkin*, F. D. Marquis**, and M. A. Meyers***

*Center of High Dynamic Pressures, Mendeleevo, Russia

**South Dakota School of Technology, USA

***University of California, USA

Received November 10, 1995

Abstract—Thermodynamic and kinetic features of chemical transformation induced by shock compression are considered using reactions of metals with silicon as a model. The mechanisms and topography of processes that occur under cylindrical geometry of dynamic loading are discussed. The electron microscopy data for the shock compression products are reported.

Chemical reactions in mixtures of solids exposed to explosion impact attract increased attention due to their extremely high rates. Studies by optical methods [1–5] showed that the conversion is considerable after ca. 10^{-7} s. Runs in which the shock compression products were conserved (ampule bearing the solid reaction mixture was cooled to room temperature for several minutes) showed that the reaction is half-completed or even goes to completeness, which is likewise unusual for such transformations.

Various mechanisms were proposed to explain the extremely high rates of solid-phase reactions (see review in [6]). The most probable of these mechanisms is to be considered below.

We selected M + 2Si systems, where M = Al, Ti, V, Nb, Ta, Cr, Mo, W, or Fe, as the subjects of study.

THERMODYNAMICS OF SHOCK COMPRESSION OF M + 2Si MIXTURES

Mixtures of powders in the molar ratio M : 2Si were exposed to an explosion impact using ammonite (detonation rate, $D_0 = 4.4$ km/s; density, $\rho_0 = 1.1$ g/cm^3; Gruneisen coefficient, $\gamma = 2.9$) and the gelatine explosive PVV-4 ($D_0 = 7.3$ km/s, $\rho_0 = 1.38$ g/cm^3, $\gamma = 3.0$). The porosity of the intact mixtures in the ampules was 0.73 ± 0.03.

The propagation of shock waves in cylindrical ampules is a complex phenomenon strongly dependent on experimental conditions and may be only approximately described. As an approximation, we accept that the Mach wave moves along the axis of the cylinder and that flat impact of ampule walls on the sample occurs at the periphery.

The size ϕ of the Mach flow was studied in cylindrical ampules of identical geometry and with similar explosives in [7, 8]. The ϕ values were $10 \pm 5\%$ of the inner ampule cross-sectional area. The temperature (and, therefore, pressure) decay from the axis to the periphery follows the square parabolic law [9] (Fig. 1).

To calculate pressures and temperatures in the media, we used additive shock adiabatic curves for compact M + 2Si mixtures, calculated using the known Hugoniot parameters (C and S):

$$U_s = C + SU_p, \qquad (1)$$

where U_s and U_p are the shock and particle velocities, respectively [10].

Table 1 summarizes the Hugoniot parameters (experimentally determined and calculated by additivity), and densities of the mixtures and their constituents (which are needed for pressure calculations).

These data were used to calculate the Hugoniot coefficients for porous mixtures by the method described in [10]; next, the axial and peripheral pressure values in cylindrical ampules were calculated in terms of the above assumptions. The calculation results are compiled in Table 2.

We proceed with estimating the residual shock compression temperatures in the axial and peripheral portions of cylindrical ampules.

The increment of the internal energy of the shock-loaded system is primarily (by 80–90%) determined by the compression of the powder until compact:

$$\Delta E = \frac{1}{2}p(V_{00} - V_0), \qquad (2)$$

where V_{00} and V_0 are the volumes of a porous and compact bodies, respectively. In this case, we may assume that the temperature at the moment of shock compression roughly equals

$$T_s = \Delta E / C_p, \qquad (3)$$

where C_p is the heat capacity.

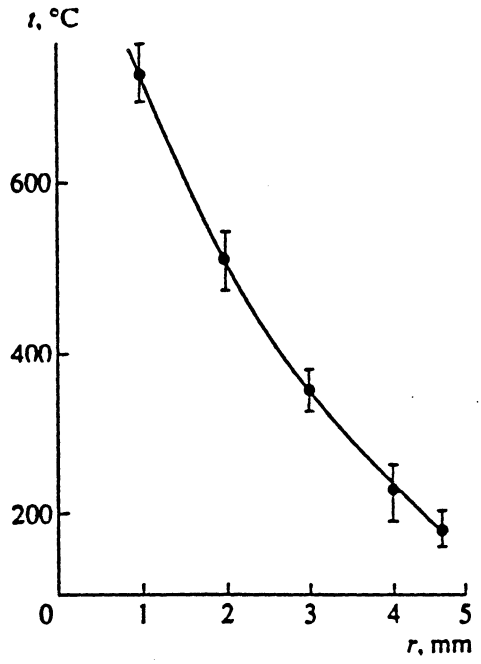

Fig. 1. Radial residual temperature distribution in a cylindrical ampule. Each data point is an arithmetic mean of 8–10 runs.

Table 3 lists the V_0, $\Delta V_{00} = V_{00} - V_0$, and T_s values for mixtures loaded to pressures listed in Table 2.

Since the calculation scheme ignores the heating of a body as the volume V_0 is reduced to V, a value dictated by the load pressure, the temperature of the off-loaded body (residual temperature, T_{res}) must not differ strongly from shock temperatures. A slight temperature depression will be caused by the consumption of the explosion energy in crushing of crystal grains and emergence of dislocations, micro-, and macrocrac the density of shock-loaded materials is reduc against the normal value; the reduction is usually a f percent. As applied to our case (27% pore volume), t explosion-induced rarefaction compensates for ~1(volume reduction upon powder consolidation, wh $V_{00} \longrightarrow V_0$. Consequently, in our case the residual te perature should be approximately 0.9 of the shock te perature (Table 4).

However, if T_{res} reaches the melting point (T_m) one or both constituent elements, the heat of melt will be absorbed, causing the system temperature decrease. If the temperature decrease is as large a reach the melting point, the mixture solidifies. Us the data on the heats of melting for the compounds (e ments) [14], we may estimate the residual temperatu making allowance for the heat consumption of melti

Given the melting points of the constituent e ments [13] and the parabolic dependence of temp ture on the distance away from the axis of the amp the dimensions of zones in which the material will r may be estimated. Assume that

$$T_{res} = a(r-x)^2 + b,$$

where r is the inner radius of the ampule, x is the ra of the heated zone, $a = (T_{ax} - T_{per})/r^2$, and $b =$ Equating $T_{res} = T_m$, we found the size of the mo zone for each constituent element. These data are s marized in Table 5. Clearly, ammonite as an explo causes only aluminum and titanium to melt in zo of 1.1 and 1.7 mm in radius, respectively. With PV as a shock-wave source, the zone of molten sil amounts to 90–100% of the sample section

Table 1. Hugoniot coefficients for metals and their mixtures with silicon

Element	M			M : 2Si		
	C, km/s	S	ρ_0, g/cm^3	C, km/s	S	ρ_0, g/cm
Al	5.333	1.356	2.698	6.096	1.298	2.436
Ti	4.937	1.04	4.505	5.915	1.193	2.993
V	5.071	1.185	6.015	6.044	1.250	3.286
Nb	4.472	1.114	8.583	5.689	1.220	4.265
Ta	3.431	1.159	16.67	5.080	1.237	6.776
Cr	5.153	1.557	7.192	6.116	1.331	3.450
Mo	5.100	1.266	10.22	6.023	1.272	4.540
W	4.015	1.252	19.26	5.519	1.268	7.128
Fe	3.664	1.79	7.875	5.516	1.369	3.590
Si	6.48*	1.275**	2.328			

* Calculated by the equation $C = (B_0/\rho_0)^{1/2}$ [11].

** Calculated by the equation $S = (B_0' + 1)/4$ [11].

Table 2. Dynamic pressures (GPa) in cylindrical ampules

Mixture composition	m	Explosive: ammonite P_{per}	ammonite P_{ax}	PVV-4 P_{per}	PVV-4 P_{ax}
Al + 2Si	0.76	3.8	8.9	9.0	35.3
Ti + 2Si	0.72	3.6	12.2	9.0	45.8
V + 2Si	0.71	3.6	13.5	9.2	49.1
Nb + 2Si	0.70	3.8	17.6	9.6	66.6
Ta + 2Si	0.70	4.0	30.1	10.3	112.2
Cr + 2Si	0.70	3.7	13.8	9.2	50.7
Mo + 2Si	0.70	3.9	18.2	10.5	70.4
W + 2Si	0.71	4.1	30.0	10.5	112.1
Fe + 2Si	0.72	3.7	14.9	9.3	55.3

(the only exception is the mixture Al + 2Si), and the zone of molten metal, 60–80% (Al and Ti melts occupy the entire cross-sectional area). At the ampule walls, the material remains mainly solid upon shock compression.

SHOCK-WAVE AND KINETIC ASPECTS OF METAL INTERACTION WITH SILICON

Comparison of the molar volumes of mixtures and compounds of composition MSi_2 [15] implies that the system volume is reduced by 28% on average upon compound formation (Table 6). This means that high pressure will promote a chemical reaction. Keeping in mind the possibility of a pressure-induced chemical reaction, we concentrate on the physical aspect of shock compression.

Since the constituent elements usually differ significantly in their wave impedance, the circulation of shock waves between particles of various hardness will cause them to be crushed. The hardest particles will be the first to crush. The difference between the particle velocities of the constituent elements will bring about the relative displacement of the constituent particles [16, 17] and provide their extensive homogenization and high rates of relative (forced) diffusion [18].

If the passage of one (faster) particle through another (slower) particle takes the period of time $\tau < 10^{-6}$ s—which occurs in the zone of high dynamic pressures—a chemical reaction in the shock wave can occur.

Next, we determine the conditions that allow the reaction to occur. Table 7 lists the particle velocities U_p of silicon and constituent metals, calculated from the Hugoniot coefficients (Table 1) by the formula

$$U_p = [(C/2S)^2 + p/S\rho]^{1/2} - C/2S. \quad (5)$$

This formula follows from equation (1) of the shock adiabatic curve and the preservation law

$$p = \rho U_s U_p. \quad (6)$$

Taking into account that here we used particles of 44 μm in diameter and assuming that the time needed for the reaction to occur is 10^{-7} s, we obtain, in accordance with [19], that

$$\tau = 2d/\Delta U_p, \quad (7)$$

where d is the particle diameter and ΔU_p is the difference between the particle velocities of the constituent elements. Therefore, the critical difference between the

Table 3. Shock temperatures (10^3 K) of M + 2Si mixtures

Mixture	V_0, cm³/mol	ΔV_{00}, cm³/mol	C_p*, kJ/mol	Ammonite T_{per}	Ammonite T_{ax}	PVV-4 T_{per}	PVV-4 T_{ax}
Al + 2Si	34.13	10.78	31.3	0.654	1.53	1.55	6.08
Ti + 2Si	34.76	13.52	36.4	0.668	2.26	1.67	8.5
V + 2Si	32.60	13.32	36.6	0.655	2.47	1.68	9.0
Nb + 2Si	34.95	14.98	34.2	0.832	3.85	2.10	14.6
Ta + 2Si	34.99	15.00	34.8	0.862	6.50	2.22	24.2
Cr + 2Si	31.55	13.44	37.6	0.661	2.47	1.64	9.1
Mo + 2Si	33.50	14.36	32.9	0.851	3.97	2.29	15.4
W + 2Si	33.67	13.75	38.5	0.732	5.36	1.87	20.0
Fe + 2Si	31.20	12.13	35.6	0.630	2.54	1.58	9.4

* Calculated from the high-temperature heat capacities of the components [12, 13].

Table 4. Residual temperatures (10^3 K) of M + 2Si mixtures

Mixture	ΔH_m, kJ/mol	Ammonite			PPV-4			
		T_{per}*	T_{ax}*	T_{ax}**	T_{per}*	T_{per}**	T_{ax}*	T_{ax}**
Al + 2Si	10.7	0.589	1.38	1.035	1.395	1.05	5.47	1.92
Ti + 2Si	14.6	0.601	2.03	1.63	1.50	1.10	7.65	4.49
V + 2Si	18.3	0.589	2.22	1.68	1.51	1.51	8.10	4.86
Nb + 2Si	31.4	0.749	3.465	1.68	1.89	1.68	13.1	9.29
Ta + 2Si	32.4	0.776	5.85	2.03	2.00	1.68	21.8	18.0
Cr + 2Si	29.7	0.595	2.22	1.68	1.48	1.48	8.19	4.73
Mo + 2Si	35.8	0.766	3.57	1.68	2.06	1.68	13.9	9.72
W + 2Si	50.3	0.659	4.82	1.68	1.68	1.68	18.0	14.1
Fe + 2Si	13.8	0.567	2.29	1.68	1.42	1.42	8.46	5.25

* Calculated by the formula $T_s \times 0.9$.

** Calculated by the relationship $(T_{res}C_p - \Delta H_m)/C_p$, where ΔH_m is the heat of melting of the most refractory constituent or of both constituents.

particle velocities of a metal and silicon, required by the shock synthesis of disilicides, is 0.88 km/s.

Table 7 and formula (7) yield the onset pressure p_r of reactions in M + 2Si mixtures under shock compression. Equations like (4) and known values p_{ax} and p_{per} (Table 2) give the dimensions of zones within which $p \geq p_r$. The appropriate p_r and r_p values are listed in Table 8 for mixtures compressed with PVV-4 charges.

Table 8 demonstrates that shock-wave synthesis can not proceed in silicon + aluminum or silicon + titanium mixtures under pressures studied. In the other mixtures (except for tungsten), zones of potential shock synthesis are considerably smaller than the zones of molten silicon and metal.

RESULTS AND DISCUSSION

The above data suggest that, in the axial portion of the 1-mm ampule, the thermodynamic parameters are high enough for both thermal and shock-wave synthesis to occur, although each reaction will follow its own mechanism and features.

In thermal synthesis, which occurs in melt and takes a rather long period of time in the residual mode, the reaction should go to completion, and resulting products should be well crystallized. Shock-wave synthesis only results in partial conversion [20], and the reaction products tend to be highly imperfect.

As was already noted, the shock-wave loading of a mixture should cause harder particles to crush, altering the grain size distribution of the constituents. In addition, differences between the particle velocities of the constituents will cause lighter (high-speed) particles to displace toward the axis and bottom of the ampule [21]. Therefore, excess silicon is expected to occur in the axial and bottom portions of the sample. This is detected by the density measurements and unit-cell parameters in case where silicides form $MSi_{2 \pm x}$ solid solutions.

Table 5. Molten zone radius (mm) in off-loaded mixtures*

Mixture	T_m, K	r	r(M)	r(Si)
Al + 2Si	932	4.3	4.8	1.6
Ti + 2Si	1155	4.15	4.65	3.6
V + 2Si	2003	4.14	2.55	3.7
Nb + 2Si	2760	4.1	3.0	4.6
Ta + 2Si	3250	4.1	3.3	4.6
Cr + 2Si	2173	4.1	2.7	3.6
Mo + 2Si	2883	4.1	3.0	4.6
W + 2Si	3650	4.14	3.0	4.6
Fe + 2Si	1808	4.15	3.3	3.6

* In calculating r(M) and r(Si), the Mach pinch radius was added to the r value from (4).

Table 6. Molar volumes (cm^3) of MSi_2 mixtures

Composition	V_{mix}	V_{comp}	$\Delta V/V_{comp}$, %
$TiSi_2$	34.76	25.22	26.6
VSi_2	32.60	22.43	31.2
$NbSi_2$	34.95	26.17	25.1
$TaSi_2$	34.99	25.95	25.8
$CrSi_2$	31.35	21.57	31.2
$MoSi_2$	33.50	24.23	27.7
WSi_2	33.67	24.48	27.3
$FeSi_2$	31.20	22.23	28.7

Table 7. Particle velocities (km/s) of the constituent elements

Element	Pressure, GPa						
	10	15	20	25	30	35	40
Al	0.60	0.86	1.09	1.30	1.51	1.70	1.88
Ti	0.41	0.60	0.77	0.94	1.10	1.25	1.39
V	0.305	0.445	0.58	0.70	0.82	0.94	1.05
Nb	0.25	0.36	0.47	0.57	0.67	0.77	0.86
Ta	0.165	0.24	0.315	0.39	0.455	0.52	0.58
Cr	0.25	0.365	0.47	0.57	0.67	0.77	0.86
Mo	0.18	0.27	0.35	0.43	0.51	0.59	0.66
W	0.12	0.18	0.24	0.295	0.35	0.40	0.45
Fe	0.30	0.43	0.55	0.655	0.76	0.855	0.95
Si	0.59	0.85	1.09	1.32	1.53	1.73	1.92

The last feature to be mentioned is that the axial Mach flow takes place 1–3 mm below the top and not in the uppermost portion of the cylindrical ampule [22, 23]. The pressures at the top are estimated in terms of off-loading of the upper stopper into the sample compressed. The p_{top} estimates and corresponding temperatures appear in Table 9. These estimates virtually linearly (see [23]) increase to peak values (p_{ax}, T_{ax}) in the nonstationary region. For these reasons, the extent of chemical conversion under shock loading in a cylindrical ampule will increase from top to bottom.

The shock compression products of Nb–Si and Mo–Si mixtures exposed to PVV-4 were studied by electron microscopy. It appeared that the reaction went to completion in the 0.5-mm zone (in the Mach pinch) and proceeded to some extent in the 1.5–2 mm zone, whereas peripheral zones contained an unreacted mixture (Fig. 2).

The electron micrographs also provide evidence of the crushing of harder particles; their interaction with silicon grains (Fig. 3); spherulite and pore formation, pointing to the occurrence of liquid-phase processes in the axial portion of the ampule (Fig. 4); and separation of a disilicide drop from the silicon surface, in accordance with the mechanism described in [24, 25].

The experimental data obtained in this work and previous studies suggest the following mechanism of reaction in M–Si systems exposed to shock waves.

At the shockfront, crystal grains are crushed to entities 100–1000 Å in size [10] and are homogenized because of their different particle velocities. In the course of forced diffusion and passage of particles through one another, a chemical reaction of the surface-layer atoms occurs behind the shockfront. Since the number of surface atoms in grains crushed by a shock wave is usually ca. 10% of the number of atoms in the grain bulk, the yield of the shock-wave reaction is also 10–30% [19].

After the pressure is released, the material melts completely by virtue of the high residual temperature in the Mach pinch, and the reaction goes to completion. Away from the ampule axis, the extent of crushing and the concentration of surface atoms capable of solid-phase reaction decrease. The shock and residual

Table 8. Zone dimensions sufficient for the pressure-assisted MSi_2 synthesis

Metal	p_r, GPa	r_p, mm	Metal	p_r, GPa	r_p, mm
Al	∞	0	Cr	31	1.6
Ti	85	0	Mo	25	2.6
V	41	0.9	W	21	3.3
Nb	31	2.1	Fe	35	1.5
Ta	23	3.1			

Table 9. Pressures and residual temperatures at the top of the ampule

M + 2Si	p_{top}, GPa	T_{top}, 10^3 K	M + 2Si	p_{top}, GPa	T_{top}, 10^3 K
Al	10.4	1.61	Cr	12.0	1.93
Ti	10.9	1.82	Mo	14.0	2.75
V	11.8	1.93	W	19.0	3.05
Nb	13.6	2.68	Fe	12.3	1.89
Ta	17.7	3.43			

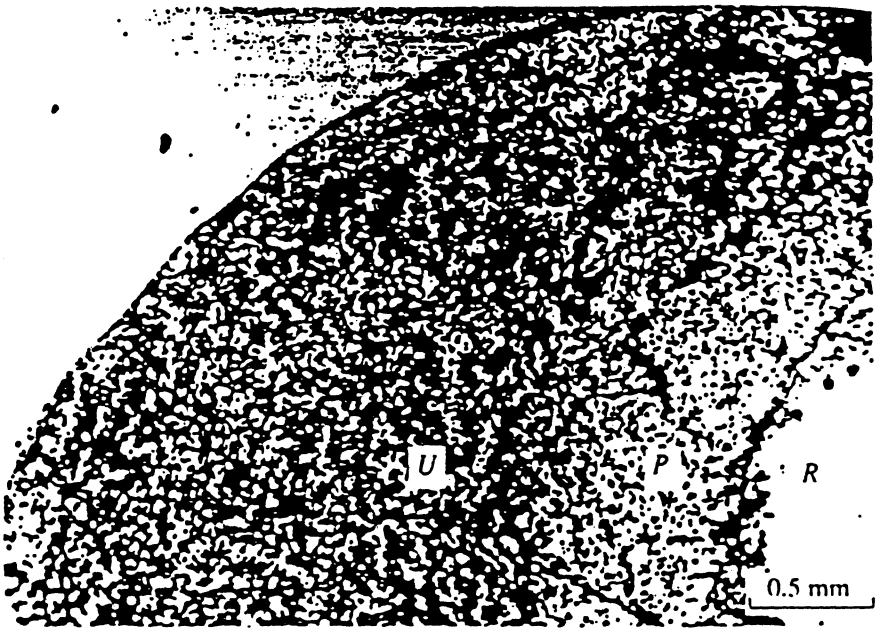

Fig. 2. Section of a cylindrical ampule containing a shock-compressed Mo + 2Si mixture: *R*, reaction was complete; *p*, reaction was partial; and *U*, unreacted portion.

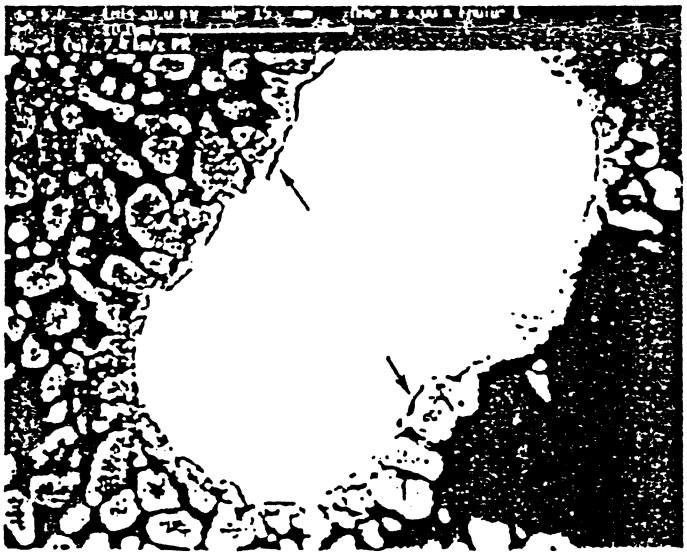

Fig. 3. Nonuniform shock-wave–induced crushing of the constituent elements: white field, silicon; gray field, molybdenum.

temperatures, as well as liquid-phase concentration also decrease in this direction, keeping the components from participating in conventional thermal synthesis.

Thus, the product topography is identical for shock and thermal syntheses, whereas the actual structure of the resulting compound should be different, depending on the reaction mechanism. The extent of chemical conversion in solid mixtures under shock compression is controlled by the diffusion rate and rate of removal of a protecting product layer from the surface of particles. In shock synthesis, the rate of removal is controlled by the difference between the particle velocities of the constituent elements and the compound; in thermal synthesis, it is controlled by the tendency of the reactants to acquire the minimum surface energy.

It remains unclear why the zones of unreacted and partially reacted mixture form a well-defined boundary at the periphery of the cylindrical ampule. The probable cause is the high activation energy of disilicide formation, which results in a dramatic decay in reaction yield

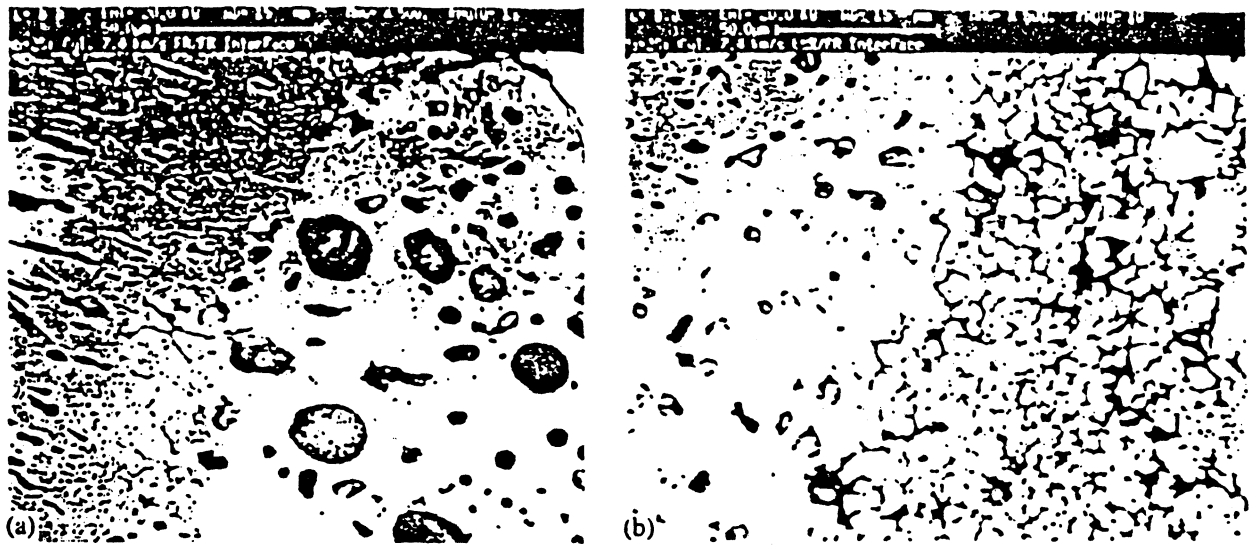

Fig. 4. Spherulite formation in the Mach pinch of preserved samples: (a) Nb + 2Si and (b) Mo + 2Si.

as temperature drops. Another probable case is that the substance flow character changes at some distance from the cylinder axis.

REFERENCES

1. Hornig, H., Kury, J., Simpson, R., *et al.*, Proc., *11th Int. Pyrotechnics Sem.*, Vail, 1986.
2. Boslough, M., *J. Chem. Phys.*, 1990, vol. 92, p. 1839.
3. Gogulya, M.F., Voskoboinikov, I.M., Dolgoborodov, A.Yu., *et al.*, *Khim. Fiz.*, 1991, vol. 10, p. 420.
4. Batsanov, S.S., Gogulya, M.F., Brazhnikov, M.A., *et al.*, *Khim. Fiz.*, 1991, vol. 10, p. 1699.
5. Gogulya, M.F., Voskoboinikov, I.M., Dolgoborodov, A.Yu., *et al.*, *Khim. Fiz.*, 1992, vol. 11, p. 244.
6. Batsanov, S.S., *Propellants, Explos., Pyrotech.*, 1993, vol. 18, p. 100.
7. Batsanov, S.S., Martynov, A.I., Strelyaev, A.E., *et al.*, Proc., *1 Vsesoyuznyi simpozium po impul'snym davleniyam* (1st All-Union Symp. on Pulse Pressures), Moscow, 1974, vol. 2, p. 45.
8. Batsanov, S.S., Andriyanova, E.E., and Lazareva, E.V., *Khim. Fiz.*, 1989, vol. 8, p. 1435.
9. Batsanov, S.S., Doronin, G.S., Koshevoi, V.P., *et al.*, *Fiz. Goreniya Vzryva*, 1968, vol. 3, p. 108.
10. Batsanov, S.S., *Effects of Explosions on Materials*, New York: Springer, 1994.
11. Ruoff, A., *J. Appl. Phys.*, 1967, vol. 38, p. 4976.
12. Baykara, T., Hauge, R., Noren, N., *et al.*, *High Temp. Sci.*, 1991, vol. 32, p. 113.
13. *Handbook of Chemistry and Physics*, Boca Raton: CRC, 1989–1990, 70th ed.
14. Batsanov, S.S., *Eksperimental'nye osnovy strukturnoi khimii* (Experimental Fundamentals of Structural Chemistry), Moscow: Izd. Standartov, 1986.
15. Bokii, G.B., *Vvedenie v kristallokhimiyu* (Introduction to Crystal Chemistry), Moscow: Mosk. Gos. Univ., 1954.
16. Deribas, A.A. and Staver, A.M., *Fiz. Goreniya Vzryva*, 1974, vol. 10, p. 568.
17. Kutsovskii, E.Ya. and Staver, A.M., *Fiz. Goreniya Vzryva*, 1975, vol. 11, p. 509.
18. Batsanov, S.S., Doronin, G.S., Klochkov, S.V., *et al.*, *Fiz. Goreniya Vzryva*, 1986, vol. 22, no. 6, p. 134.
19. Batsanov, S.S., Gogulya, M.F., Brazhnikov, M.A., *et al.*, *Fiz. Goreniya Vzryva*, 1994, vol. 30, no. 3, p. 107.
20. Gogulya, M.F. and Brazhnikov, M.A., *Khim. Fiz.*, 1994, vol. 13, no. 11, p. 90.
21. Batsanov, S.S. and Maksimov, I.I., *Khim. Fiz.*, 1990, vol. 9, p. 1274.
22. Adadurov, G.A., Dremin, A.N., and Pershin, S.V., *Fiz. Goreniya Vzryva*, 1967, vol. 3, p. 281.
23. Doronin, G.S., Stupnikov, V.P., Roman'kov, V.V., *et al.*, *Zh. Tekh. Fiz.*, 1973, vol. 43, p. 1059.
24. Yu, L.H. and Meyers, M.A., *Shock-Wave and High-Strain-rate Phenomena in Materials*, Meyers, M.A., Murr, L.E., Staudhammer, K.P., and Dekker, M., Eds., New York, 1992, p. 93.
25. Vecchio, K.S., Yu, L.H., and Meyers, M.A., *Acta Metall. Mater.*, 1994, vol. 42, p. 701.
26. Meyers, M.A., Yu, L.H., and Vecchio, K.S., *Acta Metall. Mater.*, 1994, vol. 42, p. 715.